$$\frac{1}{d_{hkl}} = \frac{1}{V}\left\{\left[h^2b^2c^2\sin^2\alpha + k^2a^2c^2\sin^2\beta + l^2a^2b^2\sin^2\gamma + 2hkabc^2(\cos\alpha\cos\beta - \cos\gamma) + 2kla^2bc(\cos\beta\cos\gamma - \cos\alpha) + 2hlab^2c(\cos\alpha\cos\gamma - \cos\beta)\right]\right\}^{1/2}, \quad (1.1.48)$$

for the triclinic case. Equation (1.1.48) simplifies considerably with symmetry to, for example,

$$\frac{1}{d_{hkl}} = \frac{\sqrt{h^2 + k^2 + l^2}}{a} \quad (1.1.49)$$

for the cubic case.

1.1.2.4. *The Ewald construction and Debye–Scherrer cones*

The Bragg equation shows that diffraction occurs when the scattering vector equals a reciprocal-lattice vector. The scattering vector depends on the geometry of the experiment, whereas the reciprocal-lattice vectors are determined by the orientation and the lattice parameters of the crystalline sample. Bragg's law shows the relationship between these vectors in a scattering experiment. Ewald developed a powerful geometric construction that combines these two concepts in an intuitive way (Ewald, 1921). A sphere of radius $1/\lambda$ is drawn following the recipe below. The Bragg equation is satisfied and diffraction occurs whenever a reciprocal-lattice point coincides with the surface of the sphere.

The recipe for constructing Ewald's sphere[2] is as follows (Fig. 1.1.9):

(1) Draw the incident wave vector $\mathbf{s}_0$. This points in the direction of the incident beam and has length $1/\lambda$.

(2) Draw a sphere centred on the tail of this vector with radius $1/\lambda$. The incident wave vector $\mathbf{s}_0$ defines the radius of the sphere. The scattered wave vector $\mathbf{s}$, also of length $1/\lambda$, points in the direction from the sample to the detector. This vector is also drawn starting from the centre of the sphere and also terminates at a point on the surface of the sphere. The scattering vector $\mathbf{h} = \mathbf{s} - \mathbf{s}_0$ completes the triangle from the tip of $\mathbf{s}$ to the tip of $\mathbf{s}_0$, both of which lie on the surface of the sphere. Thus the surface of the sphere defines the locus of points in reciprocal space where the scattering vector in our experiment may possibly lie.

(3) Draw the reciprocal lattice with the origin lying at the tip of $\mathbf{s}_0$.

(4) Find all the places on the surface of the sphere where reciprocal-lattice points lie. This gives the set of points in reciprocal space where the expression $\mathbf{h} = \mathbf{h}_{hkl}$ may possibly be satisfied in our experiment.

This construction places a reciprocal-lattice point at one end of $\mathbf{h}$. The other end of $\mathbf{h}$ lies on the surface of the sphere by definition. Thus, Bragg's law is only satisfied when another reciprocal-lattice point coincides with the surface of the sphere. Diffraction can be envisaged as beams of X-rays emanating from the sample in these directions. In order to detect the intensity of these diffracted beams, one simply moves the detector to the right position. Any vector between two reciprocal-lattice points has the potential to produce a Bragg peak. The Ewald-sphere construction indicates which of these possible reflections are experimentally accessible.

[2] For practical reasons, plots of the Ewald 'sphere' are circular cuts through the sphere and the corresponding slice of reciprocal space.

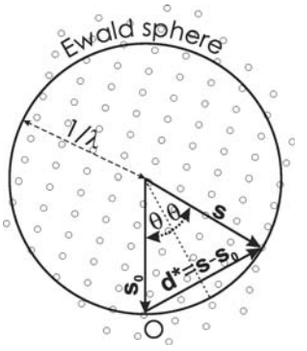

Figure 1.1.9
Simplified representation of the Ewald-sphere construction as a circle in two dimensions. O marks the origin of reciprocal space. The vectors are defined in the text. [Reproduced from Dinnebier & Billinge (2008) with permission from the Royal Society of Chemistry.]

Changing the orientation of the crystal reorients the reciprocal lattice, bringing different reciprocal-lattice points onto the surface of the Ewald sphere. In a single-crystal experiment it is necessary to repeatedly reorient the crystal to bring new reciprocal-lattice points onto the surface of the Ewald sphere, and then to reorient the detector in such a way as to measure the scattering from each particular reflection on the surface. This is done in a highly automated fashion these days. Once a diffraction pattern has been indexed so that the lattice vectors and the orientation matrix (the relation of the lattice vectors to the laboratory coordinate frame) are found, then all of the diffractometer settings that are required to collect all the Bragg peaks are fully determined and this process can be accomplished automatically.

In this chapter we are considering scattering from powders. An ideal powder contains individual crystallites in all possible orientations with equal probability. The powder experiment is equivalent to placing a detector at a fixed position and rotating a single crystal through every orientation, spending an equal amount of time in each orientation. The first powder experiment was reported by Debye & Scherrer in 1916, and independently by Hull in 1917. In the Ewald construction, this is the same as

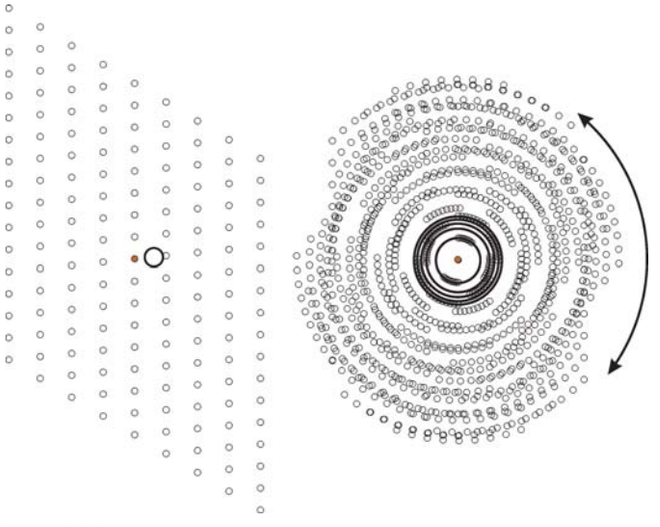

Figure 1.1.10
Illustration of the reciprocal lattice associated with a single-crystal lattice (left) and a large number of randomly oriented crystallites (right). A real powder consists of so many grains that the dots of the reciprocal lattice form into continuous lines. [Reproduced from Dinnebier & Billinge (2008) with permission from the Royal Society of Chemistry.]

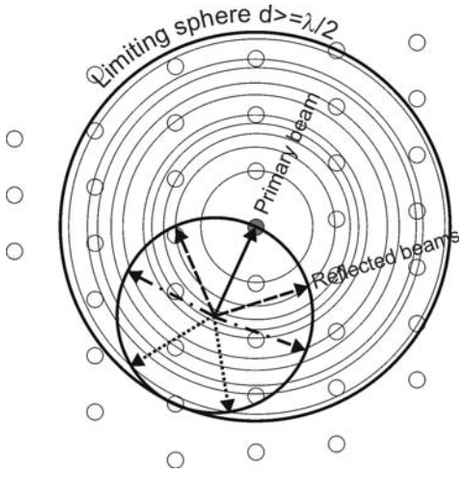

Figure 1.1.11
Simplified representation of the Ewald-sphere construction as a circle in two dimensions. Illustration of the region of reciprocal space that is accessible in a powder diffraction experiment. The smaller circle represents the Ewald sphere. As shown in Fig. 1.1.10, a powder sample has crystallites in all possible orientations, which is modelled by rotating the reciprocal lattice to sample all orientations. An equivalent operation is to rotate the Ewald sphere in all possible orientations around the origin of reciprocal space. The volume swept out is the region of reciprocal space accessible in the experiment. [Reproduced from Dinnebier & Billinge (2008) with permission from the Royal Society of Chemistry.]

smearing out every reciprocal-lattice point over the surface of a sphere centred on the origin of reciprocal space. This is illustrated in Fig. 1.1.10. The orientation of the $\mathbf{d}^*_{hkl}$ vector is lost and the three-dimensional vector space is reduced to one dimension with the independent variable being the modulus of the vector $\left|\mathbf{d}^*_{hkl}\right| = 1/d$.

These spherical shells intersect the surface of the Ewald sphere in circles. A two-dimensional projection is shown in Fig. 1.1.11. Diffracted beams can be envisaged as emanating from the sample in, and only in, the directions where the thin circles from the smeared reciprocal lattice intersect the thick circle of the Ewald sphere. A few representative diffraction beams are indicated by the dashed, dotted and dash-dotted arrows.

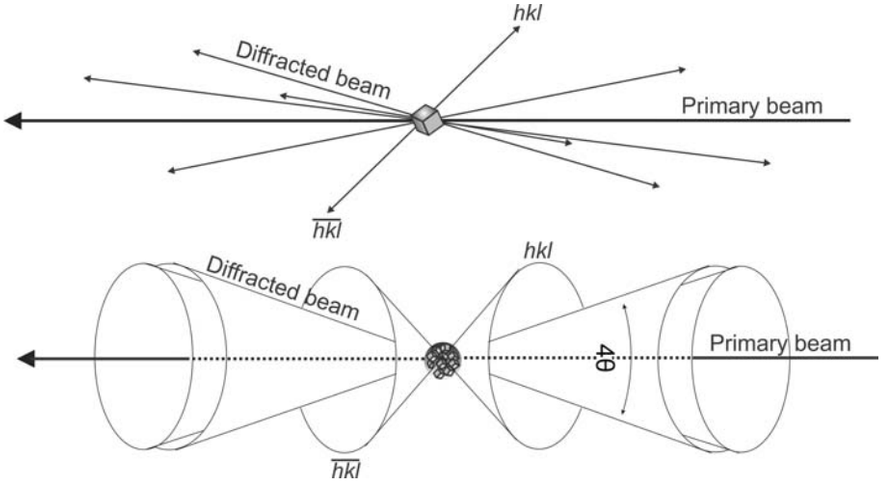

Figure 1.1.12
Comparison between the scattered beams originating from a single crystal (top) and a powder (bottom). For the latter, some Debye–Scherrer cones are drawn in reciprocal space. [Reproduced from Dinnebier & Billinge (2008) with permission from the Royal Society of Chemistry.]

The reflections from planes with the smallest d-spacing that are accessible in the experiment are determined by the diameter of the Ewald sphere, which is $2/\lambda$. In order to increase the number of reflections that can be detected, one must decrease the incident wavelength. In the case of an energy-dispersive experiment such as a time-of-flight neutron powder diffraction experiment, which makes use of a continuous distribution of wavelengths from λ_{min} to λ_{max} at fixed angle, all reflections that lie in the cone-shaped region of reciprocal space between the two limiting Ewald spheres at $2/\lambda_{min}$ and $2/\lambda_{max}$ will be detected.

As mentioned above, in a powder the reciprocal-lattice points get smeared into a spherical surface, which intersects the Ewald sphere as a circle. This means that, in three dimensions, the resulting diffracted radiation associated with the reflection *hkl* forms a cone emanating from the sample on an axis given by the direct beam, the so-called Debye–Scherrer cone. Different reciprocal-lattice points, at different values of $1/d_{hkl}$, give rise to coaxial cones of scattering. This is illustrated in Fig. 1.1.12.

The smearing of reciprocal space in a powder experiment makes the measurement of a powder diffraction pattern easier than the measurement of a set of single-crystal data, because the sample does not have to be repeatedly re-oriented, but this comes at the cost of a loss of information. At first sight the loss of information seems to be the directional information about the points in the reciprocal lattice. However, once the lattice is indexed (*i.e.* its basis vectors are known) the directional information in the pattern can be recovered without difficulty, which is why three-dimensional structures can be determined from the one-dimensional diffraction information in a powder pattern. The loss of information comes from the fact that reflections from lattice planes whose vectors lie in different directions but which have the same d-spacing overlap. These reflections cannot be resolved by the measurement and so the intensity in each of the peaks is not known. The peak-overlap problem becomes increasingly worse with increasing scattering angle as the number of diffraction planes in a particular d-spacing range increases and their separation decreases.

Some of these overlaps are dictated by symmetry (systematic overlaps) and others are accidental. Systematic overlaps are less problematic because the number of equivalent reflections (the multiplicity) is known from the symmetry, and, by symmetry, each of the overlapping peaks has the same intensity. For highly crystalline samples, the number of accidental overlaps can be reduced by making measurements with higher resolution, since this allows similar but not identical d-spacings to be separated.

To obtain the maximum amount of information, a spherical-shell detector would be desirable, although this is currently impractical. Often, a flat two-dimensional detector, either film, an image plate or a charge-coupled device (CCD), is placed perpendicular to the direct beam, or offset to one side to increase the angular range of the data collected. In this case, the Debye–Scherrer cones appear as circles, as shown in Fig. 1.1.13, or as ellipses if the detector is at an angle to the direct beam.

For an ideal powder, the intensity distribution around the rings is uniform. In a traditional powder diffraction experiment using a point detector, for example a scin-

tillator detector behind a receiving slit that defines the angular resolution of the measurement, at each position the detector samples a point on the two-dimensional diffraction pattern shown in Fig. 1.1.13. As the detector is moved to higher 2θ angles the locus of the points that are sampled is a horizontal or vertical (depending on whether the detector is moving in the horizontal or the vertical plane) line across the two-dimensional image. The intensity that is detected is low except where the detector crosses the circles of high intensity. This type of measurement is preferred for obtaining the highest resolution, especially if a highly perfect analyser crystal is used instead of a slit for defining the angle of the scattered beam. However, if the full rings, or fractions of them, are detected with two-dimensional detectors, the counting statistics can be improved enormously by integrating azimuthally around the rings at constant $|\mathbf{h}|$. This mode is becoming very popular for time-resolved, *in situ* and parametric studies where rapid throughput is more important than high resolution. It is also useful for samples that are weakly scattering and for nanometre-sized crystals or defective crystals, which may not show sharper peaks even when measured at higher resolution.

If the powder is non-ideal, the intensity distribution around the ring is no longer uniform, as illustrated in the right part of Fig. 1.1.13, and a one-dimensional scan will give arbitrary intensities for the reflections. To check for this in a conventional measurement it is possible to measure a rocking curve by keeping the detector positioned so that the Bragg condition for a reflection is satisfied and then taking measurements while the sample is rotated. If the powder is ideal, *i.e.* it is uniform and fine-grained enough to sample every orientation uniformly, this will result in a constant intensity as a function of sample angle, while large fluctuations in intensity will suggest a poor powder average. To improve powder statistics, powder samples may be rotated during a single measurement exposure, both for conventional point measurements and for measurements with two-dimensional detectors. Additional averaging of the signal also occurs during the azimuthal integration in the case of two-dimensional detectors. Outlier intensities can be identified and excluded from the integration. On the other hand, the intensity variation around the rings can give important information about the sample, such as preferred orientation of the crystallites or texture.

The d-spacings that are calculated from a powder diffraction pattern will include measurement errors, and it is important to minimize these as much as possible. These can come from uncertainty in the position of the sample, the zero point of 2θ, the angle of the detector or the angle of a pixel on a two-dimensional detector, uncertainties in the wavelength and so on. These effects will be dealt with in detail in later chapters. These aberrations often have a well defined angular dependence which can be included in fits to the data so that the correct underlying Bragg-peak positions can be determined with high accuracy.

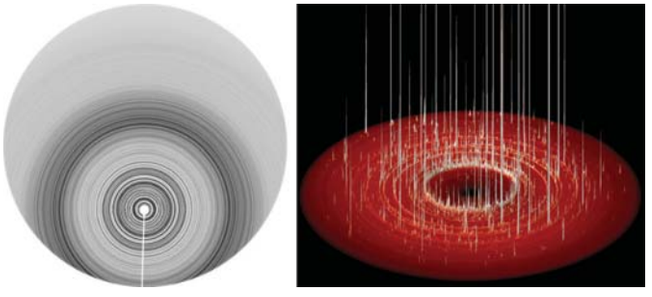

Figure 1.1.13
Left: Debye–Scherrer rings from an ideal fine-grained powder sample of a protein (courtesy Bob Von Dreele). Right: perspective view of Debye–Scherrer rings from a grainy powder sample of $BiBO_3$ at high pressure in a diamond anvil cell.

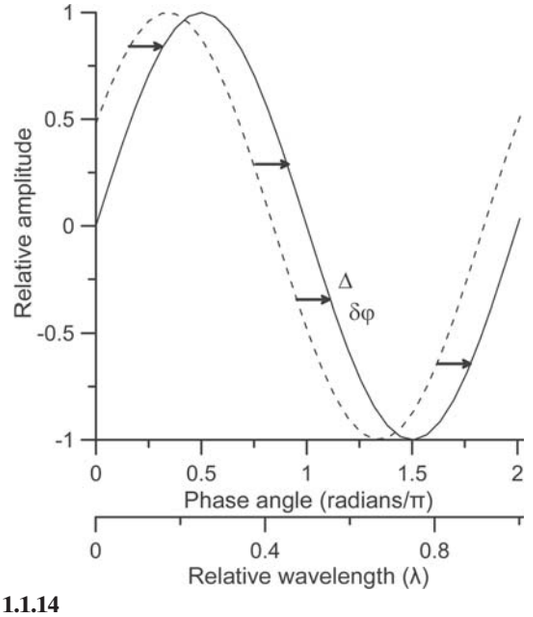

Figure 1.1.14
Graphical illustration of the phase shift between two sine waves of equal amplitude. [Reproduced from Dinnebier & Billinge (2008) with permission from the Royal Society of Chemistry.]

1.1.3. The peak intensity

1.1.3.1. *Adding phase-shifted amplitudes*

Bragg's law gives the *positions* at which diffraction by a crystal will lead to sharp peaks (known as Bragg peaks) in diffracted intensity. We now want to investigate the factors that determine the intensities of these peaks.

X-rays are electromagnetic (EM) waves with a much shorter wavelength than visible light, typically of the order of 1 Å (= 10^{-10} m). The physics of EM waves is well understood and excellent introductions to the subject are found in every textbook on optics. Here we briefly review the results that are most important in understanding the intensities of Bragg peaks.

Classical EM waves can be described by a sine wave of wavelength λ that repeats every 2π radians. If two identical waves are not coincident, they are said to have a phase shift, which is either measured as a shift, Δ, on a length scale in units of the wavelength, or equivalently as a shift in the phase, $\delta\varphi$, on an angular scale, such that

$$\frac{\Delta}{\lambda} = \frac{\delta\varphi}{2\pi} \Rightarrow \delta\varphi = \frac{2\pi}{\lambda}\Delta. \qquad (1.1.50)$$

This is shown in Fig. 1.1.14.

The detected intensity, I, is proportional to the square of the amplitude, A, of the sine wave. With two waves present that are coherent and can interfere, the amplitude of the resultant wave is not just the sum of the individual amplitudes, but depends on the phase shift $\delta\varphi$. The two extremes occur when $\delta\varphi = 0$ (constructive interference), where $I \simeq (A_1 + A_2)^2$, and $\delta\varphi = \pi$ (destructive interference), where $I \simeq (A_1 - A_2)^2$. In general, $I \simeq \left[A_1 + A_2 \exp(i\delta\varphi)\right]^2$. When more than two waves are present, this equation becomes

references